

TECHNICAL NOTE

Enhanced Damping in Long Slender End Mills

John C. Ziegert, Charles Stanislaus, and Tony L. Schmitz, Dept. of Mechanical and Aerospace Engineering, University of Florida, Gainesville, Florida, USA
Robert Sterling, The Stellar Group, Jacksonville, Florida, USA

Abstract

The limiting chatter-free depth of cut in milling is dependent on the dynamic stiffness of the tool/holder/spindle system. A method for increasing the dynamic stiffness by providing additional damping is demonstrated. The proposed damper is a multi-fingered cylindrical insert placed in an interior bore located inside conventional milling cutters. Spindle rotation forces these flexible fingers against the inner surface of the tool, and bending of the tool during cutting dissipates energy through friction, leading to improved damping and dynamic stiffness. This paper presents an analytical model of the damper, experimental measurements of tool response, and comparison between stable cutting depths using both a conventional tool and one with the damping insert.

Keywords: High-Speed Milling, Stability, Damping

Introduction

For a milling operation, the limiting depth of cut for stable, chatter-free machining is essentially determined by the dynamic stiffness of the most flexible mode of vibration of the tool/holder/spindle system (Tlustý and Poloček 1965; Tlustý 1985; Tobias 1965; Koenigsberger and Tlustý 1967; Merritt 1965; Kegg 1965). In general, if the dynamic stiffness of the most flexible mode can be increased by some multiple, the chatter-free depth of cut at any speed, and the resulting material removal rate (MRR), will increase by the same multiple. The dynamic stiffness is computed as the product of the modal stiffness, k , and the modal damping ratio, ζ . Both quantities are equally important for chatter stability.

The modal stiffness, k , is generally determined by the overall geometry (length, diameter) of the cutter body, and by its material properties, although the boundary conditions imposed by the holder/tool interface can also be important (Smith, Winfough, and Halley 1998; Davies et al. 1998; Halley et al. 1999; Schmitz and Donaldson 2000; Schmitz and Davies 2001; Schmitz et al. 2001). For many high-speed milling (HSM) applications, particularly in aero-

space, it is necessary to produce deep pockets with small radii in the corners. This often dictates the use of long, slender, and relatively flexible tools. Typical tooling used for HSM of aluminum aircraft components is 18 mm diameter and up to 200 mm of overhang. Little can be done to increase the tool stiffness in this situation. However, the damping is typically very low, usually 1% or less. Increasing the damping will have the same effect on chatter stability as increasing the stiffness. Thus, high-speed milling productivity may be improved if the damping typically seen in cutting tools can be increased significantly.

Centrifugal Damper Concept

The goal of this research is to increase the damping in end mills used for high-speed milling by the addition of internal features into the tool. The increased damping is achieved by hollowing the tool body and inserting a multi-fingered damper into the center opening, as shown in *Figure 1*. The fingers on the damper insert are created by cutting axial slits along most of the length of a cylinder whose outer diameter matches the inner diameter of the tool body, thus forming multiple fingers (similar to a sliced pie). A damper may also be inserted into a conventional solid end mill that has a blind hole in the non-fluted end.

When the tool bends, the neutral surface of the outer cylindrical tool body is located on the tool centerline. However, the fingers will bend with their neutral surfaces passing through their own centroids. The net result is that the axial strain experienced on the outer surface of the fingers will be different than the axial strain experienced on the inner surface of the tool body, causing a relative sliding between them. When the tool rotates at high speed, large centrifugal forces press the fingers against the inner surface of the tool body, creating Coulomb frictional losses. The working principle of this 'centrifugal damper' is similar to the 'replicated internal shear damper' developed by Slocum (1992) and Marsh and Slocum (1996) for machine tool structural elements—except that energy losses arise due to Coulomb friction rather than due to viscous shear.

This paper is an expanded version of an original work published in the Transactions of NAMRI/SME, Vol. 32, 2004.

technical note



Figure 1
 Hollow Tool Body and Multi-Fingered Damper Insert

Of course, when the center section of a tool is removed, the stiffness will decrease. This stiffness loss must, at minimum, be compensated by increases in the damping ratio provided by the centrifugal damper. However, the stiffness loss is minimal for holes of reasonable size. For example, in the tools developed for this work, the diameter of the central hole is one-half the outer diameter of the tool body, which reduces the bending stiffness of the tool by only 7%.

Analytical Model

The geometry of the internal damper is shown in *Figure 2*. Here, r_1 , r_2 , and r_3 represent the inside radius of the damper insert, the outer radius of the damper insert (and the inside radius of the tool body), and the outside radius of the tool body, respectively. The perpendicular distance from the neutral surface of the tool body to the neutral surface of the i th damper finger is d_i . The figure shows only one finger for simplicity; in reality an array of n such identical fingers would make up the damping insert, as shown in *Figure 3*.

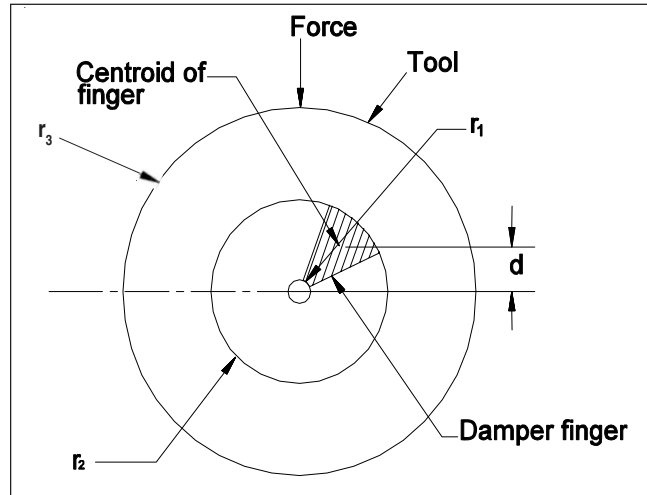


Figure 2
 Geometry of Tool Body and Damper Insert

The damping caused by the structure is due to the principle of axial shear in layered beams. Members of a composite beam that are not securely fixed together will slide over each other in proportion to the distance between their neutral axes. The tool will be modeled as a non-rotating cantilever beam of length L with a static load, F , applied to the free end.

The goal of the model is to compute the frictional work done by the sliding of the internal fingers on the inner surface of the tool body as it deflects under the action of an external end load, F . The analysis is similar to that presented in Marsh and Slocum (1996). The deflection, Δ , of the tool body and the i th damper finger is the same. Denoting the tool body as b and the fingers as f_i , and where E and I are the modulus of elasticity and the second moment of area of the cross sections, respectively, the deflection, Δ , at the tip is given by:

$$\Delta = \frac{F_b}{6E_b I_b} (-x^3 + 3xL^2 - 2L^3)$$

$$\Delta = \frac{F_{f_i}}{6E_{f_i} I_{f_i}} (-x^3 + 3xL^2 - 2L^3) \quad (1)$$

where F_b is the portion of the applied force required to deflect the tool body, and F_{f_i} is the portion required to deflect the i th finger. Because the sum of the forces on the body and the fingers must equal the total applied load:

$$F = F_b + \sum_{i=1}^n F_{f_i} \quad (2)$$

technical note

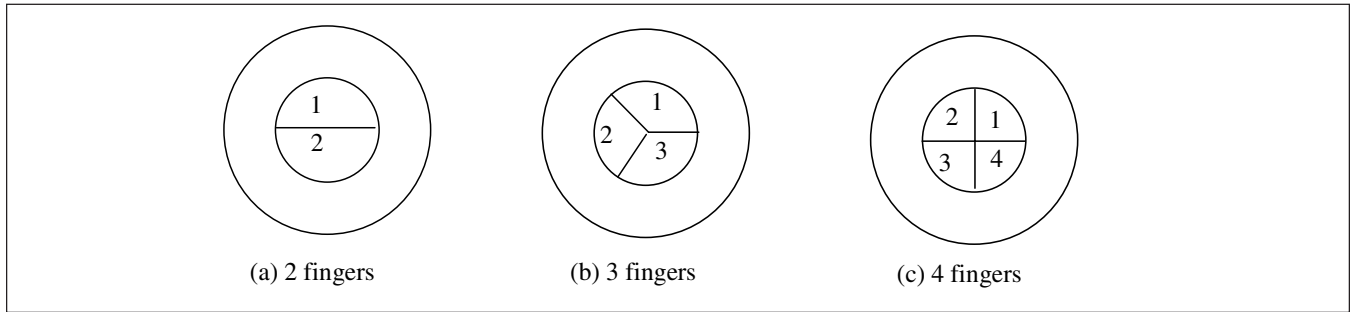


Figure 3
End View of Damper Inserts with Varying Number of Fingers

Combining Eqs. (1) and (2) yields:

$$\frac{F_b}{E_b I_b} = \frac{F}{E_b I_b + \sum_{i=1}^n E_{f_i} I_{f_i}} \quad (3)$$

The axial displacement, δ_b , of a point on the inner surface of the tool body, at any point x along the tool axis, is obtained by integrating the strains obtained from the force expressions. The distance from the neutral axis (centerline) of the tool body to the point of interest is $d + y$, where d is defined as the distance from the neutral surface of the tool body to the neutral surface of the finger (Figure 4).

$$\delta_b(x) = \int_x^L \epsilon_x dx = \int_x^L \frac{F_b x (d_i + y)}{E_b I_b} dx$$

$$\delta_b(x) = \frac{F (d_i + y) (L^2 - x^2)}{2 \left[E_b I_b + \sum_{i=1}^n E_{f_i} I_{f_i} \right]} \quad (4)$$

The axial displacement of a point on the surface of the i th finger is obtained in the same manner except that the distance from the neutral axis of the finger to the point in question is y .

$$\delta_{f_i}(x) = \int_x^L \epsilon_x dx = \int_x^L \frac{F_{f_i} x y}{E_{f_i} I_{f_i}} dx$$

$$\delta_{f_i}(x) = \frac{F y (L^2 - x^2)}{2 \left[E_b I_b + \sum_{i=1}^n E_{f_i} I_{f_i} \right]} \quad (5)$$

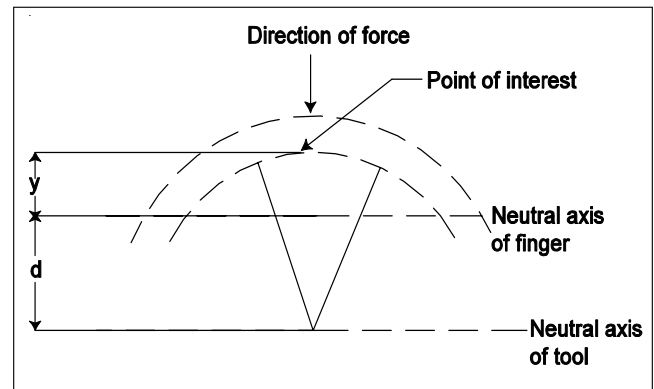


Figure 4
Location of Points on Sliding Surface

The relative displacement of a point on the inner surface of the tool body and a point on the i th finger is then:

$$\delta_b(x) - \delta_{f_i}(x) = \frac{F d_i (L^2 - x^2)}{2 \left[E_b I_b + \sum_{i=1}^n E_{f_i} I_{f_i} \right]} \quad (6)$$

Note that the relative displacement is independent of the y distance to the point. All points on the surface of the finger at an axial location x have the same relative displacement, which is proportional to the distance from the finger's neutral axis to the neutral axis of the tool body.

The friction work done by the sliding of the surface of the finger relative to the inner surface of the tool body is dependent on the pressure, P , between these two surfaces and the coefficient of friction, μ . Although this model is for a stationary beam under a bending load, it is assumed that there is an interface pressure equal to that which would occur if the tool were rotating at speed ω . In this case, the total centrifugal force on the finger will be computed and then it will be assumed that force is uniformly distributed

technical note

over the surface area of the damper finger to obtain a contact pressure, P . The total friction work of the i th finger is then obtained by integrating the product of friction stress and relative displacement over the tool length.

$$W_i = \mu P \int_0^L \frac{F d_i (L^2 - x^2)}{2 \left[E_b I_b + \sum_{i=1}^n E_{f_i} I_{f_i} \right]} dx \quad (7)$$

Finally, the total friction work is obtained by summing the work done by all the damper fingers.

$$W_{tot} = \sum_{i=1}^n \frac{L^3 \mu P F d_i}{3 \left(E_b I_b + \sum_{i=1}^n E_{f_i} I_{f_i} \right)} \quad (8)$$

This model represents a stationary, cantilever beam undergoing a deflection due to a constant force. It is understood that the cutting tool with a centrifugal damper will be rotating and that the resulting deflections and damping will depend on the dynamic response of the system and cutting conditions. However, this simple model is used to compare the frictional work when the number of fingers and internal radius are altered. The model assumes that the axial stiffness of the damper fingers is sufficiently large so that slipping does occur at the interface; that is, the axial frictional forces do not simply stretch or compress the damper finger along with the inner surface of the tool body.

Figure 5 shows the effect of the number of damper fingers on the frictional work for a tool with a 19 mm outside diameter and 100 mm length. The applied force was 100 N, and the tool and damper were made of steel with $E = 200$ GPa. Although the tool body is modeled as a hollow cylinder, the actual wall thickness must be sufficient to allow flutes to be ground into the surface. For this reason, the inside diameter of the tool body was taken to be 9.5 mm. The inner radius of the damper fingers is assumed to be zero for this analysis. As expected, for a damper with one finger (that is, a solid cylindrical insert), no frictional work is done because the neutral surface of the tool body and damper finger are coincident. Increasing the number of fingers from two to three significantly increases the damper performance. It can be seen that little is gained by using more than eight fingers.

There is a dip in the frictional work when the number of fingers is increased from three to four. This is caused by the use of zero degrees (positive x axis) as the starting

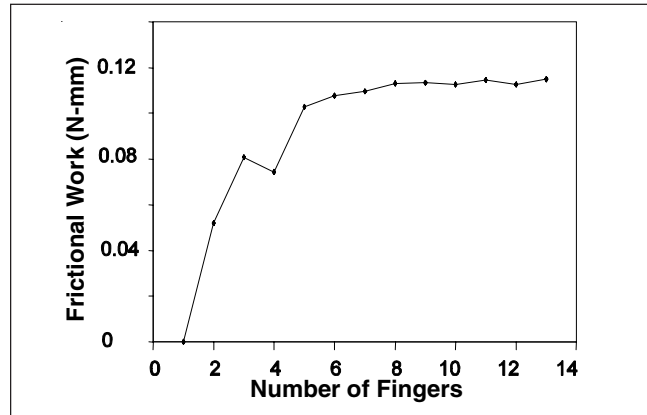


Figure 5
 Effect of Number of Fingers on Friction Work

angle of the first finger. At this orientation, the neutral axes of a three-fingered damper are arranged in such a way that it does slightly more work than a four-fingered damper arranged in the same orientation.

The effect of the internal radius of the damper insert was also investigated with this model. The internal radius of the damper was varied between 0 mm and 4 mm. Figure 6 shows that varying the center hole size results in little change in the frictional work, provided the hole diameter is less than approximately 30% of the outside diameter of the damper. Therefore, an inner hole in the damper should be added only if it simplifies manufacture.

Experimental Results

Modal Testing

To experimentally test the performance of the damper insert, two end mills were constructed. The tools were made of high-speed steel with 19.05 mm outer diameter, 125 mm length, and had three cutting flutes. Their external geometry was identical. One of the tools had an internal blind hole of 9.5 mm diameter with a length of 105 mm. The blind hole allowed cutting edges to be ground on the end of the tool. Modal testing was performed on the solid and hollow end mills, and later the damper was inserted into the hollow tool, which was measured again.

The damper insert had eight fingers and was constructed from a 9.5 mm diameter tungsten carbide blank. The diameter of the damper insert was such that the solid portion provided a light press fit into the tool body. The damper insert was slit down 76 mm of its 105 mm length by wire electrodischarge machining in order to form the separate fingers. Figure 7 shows a photograph of an end

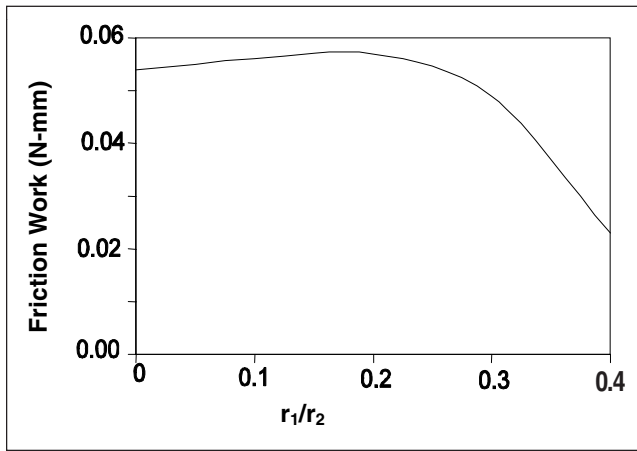


Figure 6
Effect of Internal Radius on Friction Work

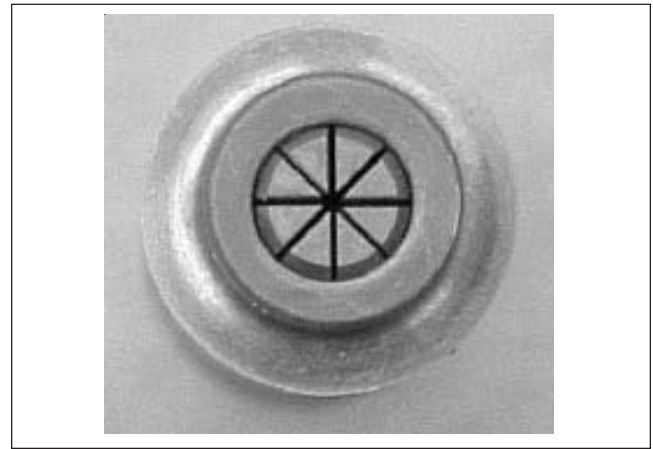


Figure 7
Model Tool Blank with the Eight-Fingered Damper

view of a hollow tool blank with the damper insert inside (tool blank has through hole).

Frequency response functions (FRFs) were measured for the solid, hollow, and hollow tool with damper under both stationary and rotating conditions. For these tests, the tool body was held in a shrink-fit style toolholder with 100 mm protruding from the end of the holder, giving an L/D ratio of 5.2:1. FRF measurements were taken for each tool at rotational speeds from 10,000 rpm to 28,000 rpm in steps of 1,000 rpm.

Due to centrifugal, gyroscopic, and, potentially, thermal effects in the rolling element spindle bearings, the dynamic response of the spindle/holder/tool system varied significantly with speed. Figure 8 shows FRF measurements obtained at 15,000 rpm in the machine x -direction for the three tools.

Mode shapes were also measured and showed that the prominent mode at approximately 1,100 Hz was primarily due to cantilever bending of the tool. Note that the natural frequencies of this mode are different for each tool. The hollow tool has both lower mass and lower stiffness than the solid tool. However, the mass drops more quickly than the stiffness when internal holes are introduced, and so the natural frequency increases as seen in Figure 8. When the damper insert is added to the hollow tool, the mass increases, but the stiffness increases very little due to the relative flexibility of the damper fingers, and thus the natural frequency decreases.

Although space limitations do not permit all of the rotating FRF measurements to be shown, Figure 9 gives typical results for the damped tool at speeds of 12,000 and 18,000 rpm, showing the changes observed in system

dynamics as spindle speed changes. The procedure used to complete the measurements and obtain the modal parameters is described more fully in Schmitz, Ziegert, and Stanislaus (2003).

Stability lobe diagrams were generated from the modal tests and were later used as a guide to choosing appropriate parameters for the cutting tests. Figure 10 shows the stability lobe diagram for the solid, hollow, and damped tools. This diagram incorporates the changing dynamic response of the system with changing rotational speed, in a procedure similar to that described by Shin (1992). Lin, Tu, and Kamman (2003) have also described methods for obtaining spindle dynamic response as a function of spindle speed.

The changing dynamics with spindle speed were incorporated by using the FRFs measured at each speed to create a separate speed-specific stability lobing diagram using standard methods described by Altintas and Budak (1995). Because the rotating FRF measurements were taken for spindle speeds ranging from 10,000 rpm to 28,000 rpm at increments of 1,000 rpm, 19 stability lobing diagrams were created for each tool. Although each of these diagrams predicted stability limits at the full range of spindle speeds, it was recognized that the variation of dynamic response with speed meant that the only valid point on each diagram was the stability limit predicted at the spindle speed at which the FRF used to create the diagram was measured. Therefore, a single data point was extracted from each of the individual diagrams and combined into the single diagram shown in Figure 10. A more detailed description of the method used to obtain the stability diagram is given in Schmitz, Ziegert, and Stanislaus (2003).

technical note

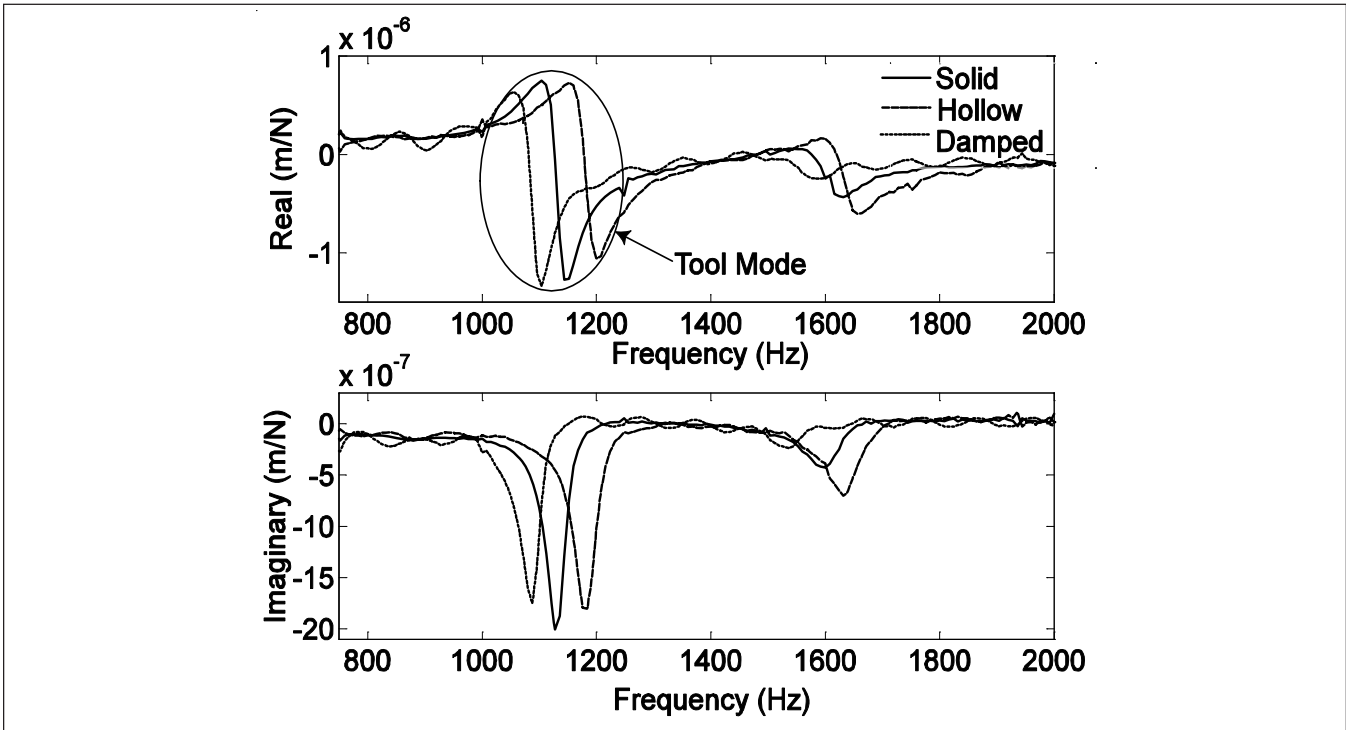


Figure 8
Rotating FRF Measurements Taken at 15,000 rpm in x-Direction

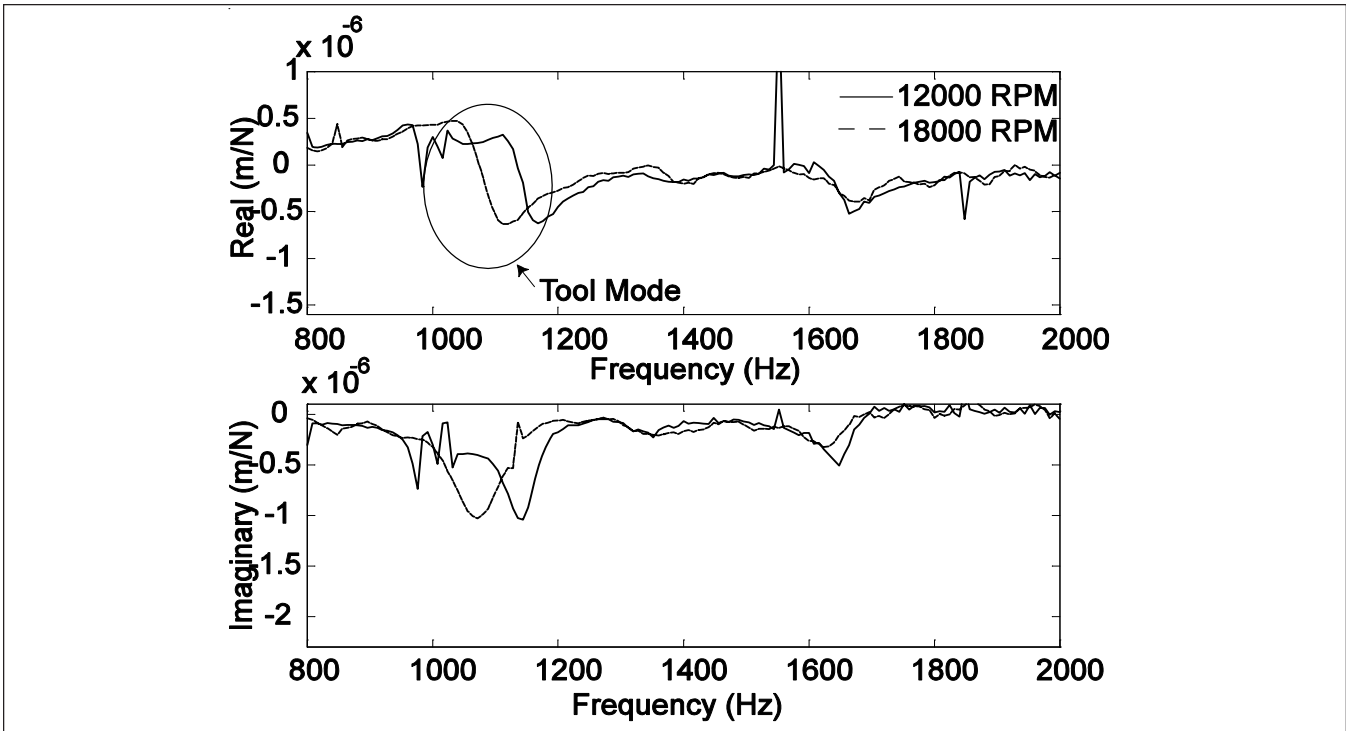


Figure 9
Changes in System Dynamics with Spindle Speed

technical note

It can be seen in *Figure 10* that the stability diagram predicts significantly deeper cuts are possible by the damped tool at spindle speeds in the 17,000 to 25,000 rpm range. The different modal frequencies of the three tools lead to a horizontal shifting of the lobes. Practically, this means that the optimum speed of operation for each tool is slightly different, and it is possible to find speeds where each of the tools outperforms the others. However, the damped tool shows the highest overall predicted stability limit.

Cutting Tests

Cutting tests were performed at the same spindle speeds as the modal testing. The testing procedure for each tool was as follows:

1. An aluminum piece was faced, deburred, clamped onto the worktable of the machine, and checked for alignment.
2. All cuts were slots obtained by feeding in the machine x -direction, using a constant chip load of 0.1 mm, that is, the feed rate was modified at each spindle speed.
3. At each speed, the axial depth of the slot was incremented in steps of 0.25 mm until chatter occurred. The onset of chatter was determined by subjective evaluation of the surface finish and by Fourier analysis of the audio signal recorded during the cut, as suggested by Delio, Tlustý, and Smith (1992).
4. Once chatter occurred, new slot depths between the stable and unstable depths were used to determine the stability limit more precisely.

The data obtained from the cutting tests are summarized in *Figure 11*. It is clear that, for most cutting speeds, the damped tool outperforms the solid tool and hollow tools. The maximum stable cut depth for the damped tool was 53% higher than for the solid tool (2.3 mm vs. 1.5 mm). The maximum stable depth of cut for the damped tool occurs at 17,000 rpm, which is lower than the 19,000 rpm speed predicted by the stability lobing diagram in *Figure 10*. The reasons for this discrepancy are unclear, but may be related to the sensitivity of the predicted lobe crossing points to damping ratio for systems with multiple modes of vibration. The FRF measurements on the rotating tools contained significant noise due to surface roughness of the tool, runout, and grounding difficulties on the rotating tool. Smoothing was achieved by modal fits assuming a system with four degrees of freedom. It is also possible that this fitting process caused a shifting of the lobe crossing positions.

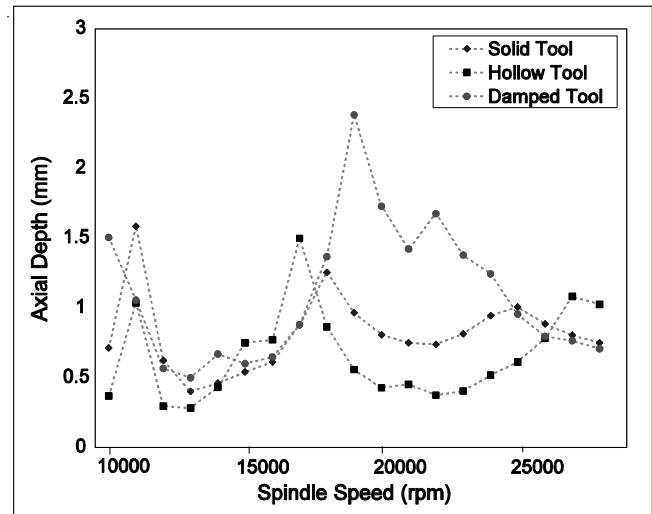


Figure 10
Stability Limits from Rotating FRF Measurements

Although the damped tool significantly outperforms the solid tool, it does not provide deeper cuts at all spindle speeds. As explained earlier, this is due to differences in natural frequencies of the three tools, and the horizontal shift in the stability lobes which result. Because the solid, hollow, and damped tools do not have the same natural frequency, the gaps between the lobes occur at different spindle speeds for the tools. This variation of the lobe positions causes the solid tool to outperform the damped tool by a small margin at some speeds.

However, in high-speed milling, the spindle speed is selected to maximize the stable MRR. When this is done, the damped tool can provide up to a 53% increase in MRR versus the conventional tool, resulting in a substantial decrease in process time and cost.

Summary

The goal of this research was to analyze and test an internal damping mechanism to help stabilize milling cutters against chatter vibrations. A simplified analytical model was developed to predict frictional work of the damper due to a static force applied to the end of the tool and was used to investigate the effects of various design parameters on the damper performance.

Based on the model results, two geometrically identical tools were produced, except for a blind internal hole in one to accommodate the damper insert. Modal testing using a hammer and capacitance probe was performed while these tools were stationary and rotating. The rotat-

technical note

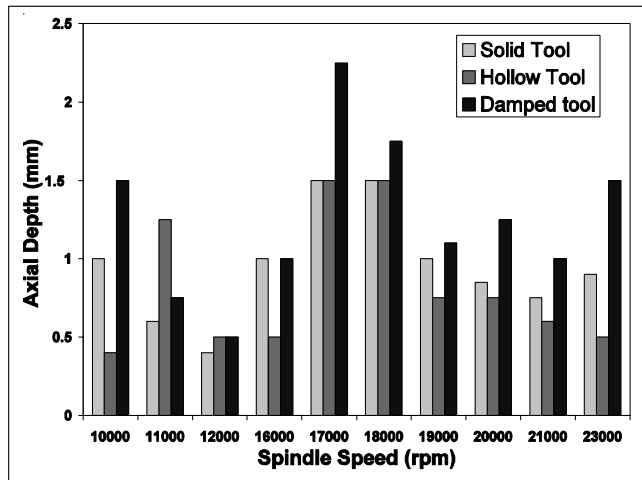


Figure 11
 Stable Cutting Depth vs. Spindle Speed

ing FRF measurements were used to create stability lobe diagrams, which predicted improved performance for the damped tool. Cutting tests showed good agreement with predictions, resulting in a 53% increase in maximum stable cutting depth for the damped tool.

Acknowledgments

This work was supported in part by NSF Grant DMI-0000009.

References

- Altintas, Y. and Budak, E. (1995). "Analytical prediction of stability lobes in milling." *Annals of the CIRP* (v44/1), pp357-362.
- Davies, M.; Dutterer, B.; Pratt, J.; and Schaut, A. (1998). "On the dynamics of high-speed milling with long, slender endmills." *Annals of the CIRP* (v47/1), pp55-60.
- Delio, T.; Tlustý, J.; and Smith, K.S. (1992). "Use of audio signals for chatter detection and control." *ASME Trans., Journal of Engg. for Industry* (v114), pp146-157.
- Halley, J.; Helvey, A.; Smith, K.S.; and Winfough, W.R. (1999). "The impact of high-speed machining on the design and fabrication of aircraft components." *Proc. of 17th Biennial Conf. on Mechanical Vibration and Noise, 1999 ASME Design and Technical Confs., Las Vegas, Sept. 12-16, 1999.*
- Kegg, R.L. (1965). "Cutting dynamics in machine tool chatter." *ASME Trans., Journal of Engg. for Industry* (v87, n4), pp464-470.
- Koenigsberger, F. and Tlustý, J. (1967). *Machine Tool Structures-Vol. I: Stability Against Chatter*. Pergamon Press.
- Lin, C-W.; Tu, J.F.; and Kamman, J. (2003). "Characterizing high-speed thermo-mechanical-dynamic behaviors of motorized machine tool spindles." *Int'l Journal of Machine Tools and Manufacture* (v43, n10), pp1035-1050.
- Marsh, E.R. and Slocum, A.H. (1996). "An integrated approach to structural damping." *Precision Engg.* (v18, n2/3).
- Merritt, H. (1965). "Theory of self-excited machine tool chatter." *ASME Trans., Journal of Engg. for Industry* (v87, n4), pp447-454.
- Schmitz, T. and Donaldson, R. (2000). "Predicting high-speed machining dynamics by substructure analysis." *Annals of the CIRP* (v49/1), pp303-308.

- Schmitz, T. and Davies, M. (2001). "Tool point frequency response prediction for high-speed machining by RCSA." *Journal of Mfg. Science and Engg.* (v123), pp700-707.
- Schmitz, T.; Davies, M.; Medicus, K.; and Snyder, J. (2001). "Improving high-speed machining material removal rates by rapid dynamic analysis." *Annals of the CIRP* (v50/1), pp263-268.
- Schmitz, T.; Ziegert, J.; and Stanislaus, C. (2004). "A method for predicting chatter stability for systems with speed-dependent spindle dynamics." *Transactions of NAMRI/SME* (v32), pp17-24.
- Shin, Y.C. (1992). "Bearing non-linearity and stability analysis in high speed machining." *ASME Trans., Journal of Engg. for Industry* (v114, n1), pp23-30.
- Slocum, A.H. (1992). *Precision Machine Design*. Englewood Cliffs, NJ: Prentice-Hall.
- Smith, K.S.; Winfough, W.; and Halley, J. (1998). "The effect of tool length on stable metal removal rate in high-speed milling." *Annals of the CIRP* (v47/1), pp307-310.
- Tlustý, J. and Poloczek, M. (1963). "The stability of the machine-tool against self-excited vibration in machining." *Proc. of Int'l Research in Production Engg. Conf., ASME, Pittsburgh, 1963*, pp465.
- Tlustý, J. (1985). "Dynamics of high-speed milling." *Handbook of High-Speed Machining Technology*, R.I. King, ed. New York: Chapman and Hall, pp48-153.
- Tlustý, J.; Smith, K.S.; and Winfough, W. (1996). "Techniques for the use of long slender end mills in high-speed machining." *Annals of the CIRP* (v45/1), pp393-396.
- Tobias, S.A. (1965). *Machine-Tool Vibration*. Glasgow, Scotland: Blackie and Sons Ltd.

Authors' Biographies

John Ziegert received his BSME from Purdue University, his MSME from Northwestern University, and his PhD in mechanical engineering from the University of Rhode Island. He began his engineering career at Pontiac Motors and, prior to joining Clemson University in 2006 as the Timken Chair in Automotive Design and Development, held faculty appointments at Roger Williams University, Brown University, the University of Hawaii, the University of Florida, and the California Institute of Technology. He joined the University of Florida in 1990 and was appointed to the Newton C. Ebaugh Chair in Mechanical Engineering in 2004. He is a registered Professional Engineer, a Fellow of the American Society of Mechanical Engineers, past president of the American Society for Precision Engineering, and currently serves as editor-in-chief of *Precision Engineering: Journal of the International Societies for Precision Engineering and Nanotechnology*. His research focuses on precision machine design and the design of instruments and systems for high-precision dimensional metrology and manufacturing.

Dr. Tony L. Schmitz is an associate professor in the Dept. of Mechanical and Aerospace Engineering at the University of Florida, where he is the director of the Machine Tool Research Center. His primary interests are in the fields of manufacturing metrology and process dynamics with current projects in high-speed machining and displacement measuring interferometry. Prior appointments include a postdoctoral fellowship followed by a mechanical engineering position at the National Institute of Standards and Technology and lecturer at Johns Hopkins University. Recent professional recognitions include the National Science Foundation CAREER award, Office of Naval Research Young Investigator award, and the Society of Manufacturing Engineers' Outstanding Young Manufacturing Engineer award. Schmitz received his PhD from the University of Florida in 1999.

Charles Stanislaus and Robert Sterling are former students of Dr. John Ziegert at the University of Florida.